# Multilayer YBa2Cu301-x/Cao.3Yo.1Ba2Cu301-x Nanocomposite Films With 2-8% BaZr03 Doping for High-Field Applications

Mohan PanthG, Mary Ann SebastianG, Di Zhang. Victor Ogunjimi, Bibek Gautam, Jie Jian, Jijie Huang, Yifan Zhang, TimotJ1y Haugan. Haiyan Wang, and Judy WuG

Abstract-High-Held •1>1>llcations require high concentn,tlonsor strong pinning centers. In this article, BaZr03 doped YBa,CuaO, (BZO/YBCO) nanocom1>0Slte Hims \\1th BZO do1ilng u1>l.o 8 vol.% were fnbri<.-ated inn mullilnyer [L) fo1nmt byinserting two10 nm thick CUo.sY0.,Ba,Cu,o,•• spacer layers in the BZO/YBCO mmocomposite films for impro,ed pinning uud enhanced critical current density $J$ at high fielcls. Signifi<."tlllt $J$ e.nhuncement was obse1wd in all the BZO/YBCO ML films or IIZO doping in the entire range ot"2-8 ,,ot.% as compared to their SL cotmtc1']))art's. At 65K, the enhancement ot"peak pinning fo1•ce density (F p,m.ru:)is 71,67,2%,and 47% for2,4,6,and 8 vol.% IIZO/YBCO Ml,films, resp<ctlvely. In addition, the *Bmex* (the location or the F,,mexl *Is* shifted cowards higher ,·alues ror BZO/YBCO ML Hims by up to 33%. lnterestlngli•, at high BZO doping or 8 ,·ol.%, lhe enhanced moduluh.-. dstrain field was found to reduce the detrimental effect of Cu ion diffusion on Tc, leading to $Jc$ enhunc."ment at n stnmg field up to 9 Tat all orie.ntntious of the mngnetk field.

*Index Terms-BZONBCO* intcl"f'nce, lattice mismatch, pinning efficiency, strain field, vo1·tex pinning.

## I. INTRODUCTION

HIGH temperature superconductor (HTS) REBa2Cu3O7., (REBCO with RE representing rare earth elemenis of Y, Er, Nd, Gd, Sm) can play a critical role in a broad variety of praclical applications including power transmission cables, lransformers, faull currenl limiters, and high field magnels [l], [21, [3], (4], [5]. High critical current density (J,) and pinning force density (Fp} in a magnetic field (8) represents the fundamental requirement for mosl of these applications [6). This has motivaled an intensive research in generating artificial pinning centers (APC) in HTS rilms through self-assembly during film growth (6), (7), [8], [9], [10), [11], [12), (13) with different morphologies of one-dimensional (1-D), 2-D, and 3-D for isolropic pinning with respect to B-field orienunions [7], [14], [15]. The APC's morphology, orientation, a11d size are shown lo be affected by the strain field initialed from the APC/HTS interface duetolattice mismatch between the two materials [14], [ I6]. In particular, ID-APCs of secondary dopa11ts like BaZ'°3 (BZO), BaHfO3 (BHO), BaS□O3 (BSO), YBa2(Nb/fa)O5, and Y20₃ in YBa2Cu3O7., (YBCO)orother REBCO haveattracted broad interesls since they can provide slrong correlated pinning at8//c-axis toaddress theweak pinning issue in layer-structured YBCO (8), (10), [14], (17). (18), [19), [20), [21), [22], [23]. Among others, BZO ID-APCs have been intensively studied afler the pioneering work by MacManus-Driscoll et al. ( IOJ since they can form as c-axis aligned arrays in a broad range of high BZO doping with areal densily proportional linearly to the BZO doping, which is important to obtain optimal pinning in applicalions targeted al specific applied magnetic fields [12], [24], [25], [26), [27], [28). However, a semicoherent BZO ID-APCNBCO interface of a high defeel concenlralion has been revealed, which has been anributed to the large lattice mismatch of ~7.7% between BZO and YBCO and hence att large strain at the BZO ID-APC/YBCO interface [16), (26), (29], [30). This defective interface has been argued 10 bean obstacle to realize the pristine pinning efficiency of the BZO ID-APCs [20], [29], [31].

In order to improve the BZO/YBCO interface and hence the pinning efficiency of BZO ID-APCs, we recently devel• oped a multilayer (ML} approach to facilitate YBCO c-axis elongation dynamically via Ca/Cu substitution on the Cu-O planes of YBCO during or immediately afler BZO ID-APCs formation. lo 2 vol.% BZO/YBCO nanocomposite ML films, the elongated c-axis to ~t.24-1.26 om has been observed, resulting in reduced BZO/YBCO lattice mismatch to 1.4% [32]. This dynamic YBCO c-axis elongation has shown to

Manuscript received 11 May 2022; revised 13 July2022:accepted 12August 2022. 03teof publication 17 August 2022; date of current version 30 August 2022.The wortof D. Zhangand H.Wang wassupported bytheU.S. NSF for the higtHesolutio11STEM effortat Purdue University uodet Gram DMR-1S6S822 and Grant OMR-2016453. This ..-..-ork was supported in pan by the National Science Foundation contracts under Grant NSF-DMR-1508494 and 1909292 and Grant NSF-Ea:S•l8W293, in part by the Air Foroe Research Laborntory Aerospaoe Systems Oirec1orate. tile Air Fo«:e Office of Scientific Rcseatth uoder Grant LRJR 14RQ08COR and Graul LRIR JSRQCORJOO. This paper was recommended by Associate Editor A. Augieri. *(ComJpo,tding 0111hors: Mohm1 Panlh: Judy \Vu.)*

Mohan Pnnth,·victor Ogunjimi, Bibek Gnutam, and Judy Wu are with the Oepartn.-.enl of Physics and Aslronomy, Uni,·ersity of Kans.as. Lawrence. KS 66045 USA (e-mail: panthm@ku.edu: victorogunjimi@ku.edu; gautam.bik@gma.il.com;jwu@k.u.edu).

Mary Ann Sebastian and 11.mothy Haugan are with the U.S. Air Force Re• searc.ll Labonllory. Ac.rospaceSystems Oi.reclC>rate. WPAFB. OH 45433 USA. a11d also with lhe UnivetSily of Dayton Research institute. Daytoo. OH 4S469 USA(e-mail:mary_ann..seba..'1.ian.J.cu@us.af.mil; timothy.haugan@us.af.mil).

Di Zhang, Jic Ji.an, Jijie Huang, Yifan Zhang, and Haiy:in Wang are with the School of Materials Engineering., Purdue Uninm••i1y, Wesl Lafayette. IN 47907 USA (e-mail: richatd2.bang1221@gmail.com: jianjie@gmail.oom: huan&ij83@mail.sysu.edu.c-n: fantonyzhang@gmail.com; h\.\l'SOgOO@pordue.edu).

This article has supplementary material provided by the au• tbots and color versions of one or more figures avaiJable at https://<loi.orglI0.1109/TASC.2022.3199306.

Digital Object Identifier I0.1109/TASC.20'2Z.3199306

prevent the deFective BZO/YBCO interface to fonn, resulting in a coherent 82O/YBCO interface together with considerably enhanced pinning. Considering Ca/Cu substitution is favored energetically on tensile-strained YBCO with since Ca ion is about 30% larger than Cu ions [331, the ML approach may be applied to 82O/YBCO nanocomposite films with higher 820 doping especially since the tensile strain is expecled Lo increase with BZO doping. In this article, we report a study on 82O/Y8COMLnattocompositeflintswith820 concentrations of up to 8 vol.%. Remarkably, enhanced *Jc* and *Fp* have been observed on all ML samples as compared to their single-layer (SL) 82O/YBCO nanocomposites counterparts.

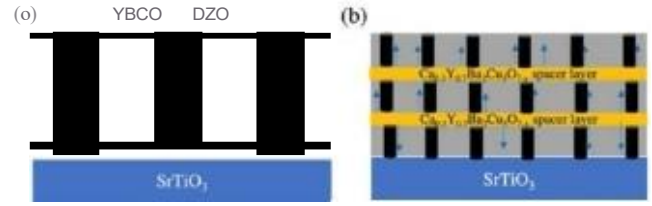


**Fig. I. Schematic description orcross-sectionalmicrostruc1uresof:(a) SLand (b) ML BZOIYBCO nanooomposite films containing the same dopingof BZO with comparnble BZO ID·APC(black) diametersandconcentration.,;. In theSL case, a tens.ile .strained YBCO column (white) is ilhL'>lr:tLcdaround each BZO 10-APCduelo lhelarb,er 820 latticeCC>nSUU\l by7.7%.**

## II. EXPERIMENTAL

8ZO/Y8CO nanocomposite ML flints and their SL counterparts were fabricated using pulsed laser deposition (PLD) on ( I00) SfTIO3 (STO) single-crystal substrates. A KrP excimer laser of wavelength ~248 nm was used for PLD with pulseenergy ~450 mJ.Forfabrication of PLD 82O/YBCO SL samples, YBCO targets containing 2, 4, 6, and 8 vol.% BZO doping, respectively, were used to obtain 2% SL, 4% SL, 6% SL, and 8% SL films, respectively. The PLD repetition rate was 8 Hz. The deposition temperature was 825 °C and the oxygen pressure was 300 mTorr. For fabrication of BZOIYBCO ML samples, att additional $Cao._3Yo._{78}a_2Cu.3O_{7\_x}$ (Ca Y-123) PLD Larget was adopted for growth of two Ca Y-123 spacers into 2, 4, 6, and 8% BZO/YBCO ML films. The spacer has an optimal thickness of ~IO nm and the PLO repetition rate of ~2 Hz based on our previotts studies (32]. The obtained 82O/YBCO ML films have a mullilayer structure with three ~50 nm thick BZO/YBCO layers separated by two ~10 nm thick CaY-123 spacers. Since the starting layer is 82O/YBCO on STO substrates, the same nucleation of BZO ID-APCs in ML and SL samples is anticipated, which means that the areal density and diameter of the BZO l D-APCs would be comparable in these two kinds of samples assuming the main effect of the two thin CaY-123 layers would trunc- te the 820 l D-APCs into threesegments of ~50 nm each in segment length [34], (35]. After the PLD deposition, the films were annealed at 500 °C in one atmospheric oxygen pressure for 30 min. It should be noted that the PLO condition For BZO/YBCO layers was optimized based on the previous studies (21], [36], [37]. The film thicknesses were measured using a Tencor P-16 profilometer. The SL and ML films have a typical thickness or 150 nm and 170 nm, respectively. Scanning transmission electron microscopy (STEM) intages undera high angleannular dark field mode were taken using a Thermo Fisher Scientific (PEI) Themis-Z transmission electron microscopy (TEM) system, which is an aberration-corrected electron microscope with the STEM resolution as small as 63 pm al an acceleration voltage or 300 kV with combined correctors. The cross-sectional TEM satnples were prepared by focused ion beam (FIB) technique using a FEI Helios Nanolab 600i Dual beam FIB/SEM system. Crystallinity and lattice parameters weredetennined using X-ray diffraction (XRD) on a Bruker 08 Discover diffractometer. In all nanocomposite satnples, c-axis-aligned ID-APCs have been confirmed with BZO I D-APC diameter ~5-6 nm [38]. For electrical transport measurement, two parallel mie-robridges with a bridge length of 500 *μm* and a width of 20 or 40 1,m were pauemed on each rilm using standard photolithography. The details of the patterning and satnple wiring for the transport measurement can be found in our previous work [32]. Briefly, Ag contact pads of ~ I mm in diameter and ~ 120 nm in thickness were deposited at room temperature through a shadow mask using de magnetron sputtering at the deposition rate of approximately 0.07 nm/sunder the argon pressure of 30 mTorr. Platinum wires or 50 *μm* in diameter were auached to the Ag pads using lncliunt. *Jc* was measttred at different applied magnetic fields of 0-9 Tin a temperature range of 65-77 Kin a Quantum Design Ever-Cool II Physical Property Measurement System. The measurement was taken at() = O" (8//c.axis) and at different orientations away from *Blie-axis (0* up to 90") in the plane perpendicular to *J* · The values were extracted by fitting the measured *1-V* curves using the formula of Voc/N. A Standard rour-probe technique was used and the *Jc* values were determined by the voltage threshold of I *μVlcm.* The *Fp* was calculated based on the equation $F_P = Iex\ 8$.Themaximum pinning force density (F,,,max) and its corresponding magnetic field (Bmax) were determined from the $F_p(8)$ curves.

## m. Resuus ANDDISCUSSION

Fig. I illustrates schematically the cross-sectional nticrostructures of 820/YBCOSL andMLfilms. The SL film contains an arrayof c-axis-aligned BZO ID-APCs (black) grownthroughout the entire film thickness of the YBCO film [see Fig. l(a)]. The defectiveYBCO coluntn of a few run in thickness around a 820 ID-APC(white)is undera tensile strainsince the laLticeconstanl or BZO is 7.7% larger than the c-axis lattice constant of YBCO. In comparison with the SL counterpart, the ML satnple [see Fig. J(b)J contains two additional CaY-123 spacers (orange) to provide sources or Ca that can diffuse into BZOIYBCO layers as shown by the dark blue arrows. The C.1/Cu substitmion is energetic-ally favorable in the tensile strained YBCO columns around the BZO l D-APCs since the Ca ion is about 30% larger than the Cu ion. The Ca/Cu substitution on the Cu-O planes of YBCO has been confirmed in a high-resolution transmission electron microscopy study on 2% BZO/YBCO ML samples, which was shown to lead to the formation of short segments of stacking faults on Cu-O planes in YBCO and elongation of the

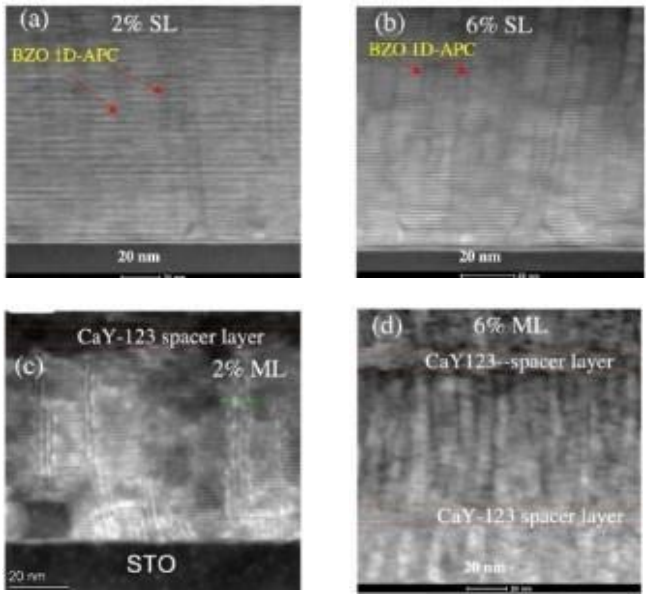


**Fig. 2.** Low magnification cross-sectional STEM images of the (a) 2% SL, (b) 6%SL (c)2% ML. and (d) 6%ML 820/YBCO nanooomposile films.

YBCO c-axis from 1.17 nm 10 up 10 1.26 nm near BZO/YBCO interface [32]. Consequently, a coherent BZO/YBCO interface can be obtained owing to the reduced BZO/YBCO lattice mismatch to ~1.4%, as shown in Fig. l(b). It should be noled that Ca/Y and Ca/Ba substitutions are also possible. Based on the elastic energy consideration, Ca/Y substitution is preferred when YBCO lattice is not under strain since the two ions have similar radii while Ca/Ba substitution would become preferred in YBCO under compressive strain [331, [39], (40], [41]. In BZO/YBCO nanocomposite films, tensile strain initiated from the BZO ID-APC/YBCO interfacecan extend toa largedistance of ~ 5-10 nm. This means I.hat Ca/Cu and Ca/Y substitulions are both possible in BZO/YBCO nanocomposite films with low BZO doping before strain field overlap occurs. While Ca/Cu substitution is more favorable near the BZO ID-APC/YBCO interface. In addition, Ca/Y substitution is well known to overdope YBCO, which may also be beneficial to balance out the detrimental effect of lattice strain on the superconductivity of the YBCO (42], [431. With increasing BZO doping, such a strain field around individual BZO ID-APCswilloverlap, which means that the entire YBCO lattice is under the tensile strain along the c-axis. Therefore, Ca/Cu substitution may provide more benefit to restoring the pinning efficiency of the BZO 1D-APCs at higher BZO doping via YBCO *c-axis* elongation.

Fig. 2(a)-(d) shows the low-magnification STEM images of 2% and 6% SL and ML BZO/YBCO films, respectively. BZO 1D-APCs can be clearly seen to be embedded in the YBCO film matrix in all four samples. In both 2% and 6% SL films, BZO I D-APCs are grown through the entire fiIm thickness. The spacing between B2O ID-APCsfor 2%and 6%SLareestimated lo be20 nm and 12 nm, respectively.In the STEM images of2% [see Fig. 2(c)J and 6% [see Fig. 2(d)] ML BZO/YBCO films, the BZO I D-APCs are truncated to segments by the caY-123 spacers while the alignment of the B2O ID-APCs is along the c-axis lhrough the entire film thickness.

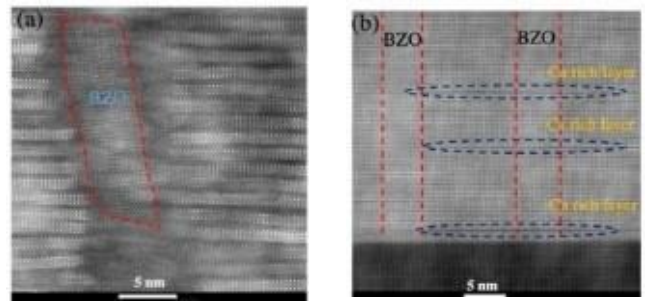


**Fig. 3.** High-resolution STEM images of (a) 2% SL and (b) 2% ML BZOIYBCO nanocornposite films. The ronnation orstacking fauJtsin the ML filmishighlightedbydotted blueovaJs. In bothfigures,thescale barsare5 nm,

Fig. 3(a) and (b) exhibits a zoom-in view of the microstructures of the 2% SL and ML B2O/YBCO samples, respectively, taken with high-resolution STE!M. Several differences can be seen clearly between the two samples. First, the B2O ID-APC/YBCO interface in the SL sample [see Fig. 3(a)) is defectivewith a largeconcentration ofdislocationson the YBCO lattice, whichagrees weU with previotLS reports[29).In addition, the YBCO laUice near the interface exhibilS a considerable distortion, indicative of a large strain initiated rrom the BZO I D-APC/YBCO interface. Finally, the morphology of lhe BZO ID-APC seems to be strongly affected as illustrated not only the nonuniform edges but also the local misalignment of the BZO I D-APC with respect lo the c-axis of YBCO. In contrast, a highly coherent BZO ID-APC/YBCO interface can be seen in the ML sample [see Fig. 3(b)J.In particular, the dislocations and latticedistortion are almost negligible near the BZO/YBCO interface. Consequently, the BZO ID-APCs look straighter than their counterparts in the SL sample with unifonn edges and align weU with the c-axis of YBCO. As shown in Fig. 3(b), a primary reason responsible for the improved microstructure in the ML sample is the fonnation of stacking faults on the Cu-O planes of YBCO (shown in blue dotted ovals}. Consequently, the YBCO lattice around these features has an elongated c-axis lallice constant up 10 1.26 nm [32]. This explains the highly coherent B2O/YBCO interface with much less obvious lattice distortion due lo U,ereduction of I.helattice mismatch to as small as~l.4%.

TheXRD *(} -2fJ*spectra taken on the SL and ML films 2, 4, 6, and 8% B2O doping, respectively, are shown in Figure SI (Supporting Material). The appearance of YBCO (001) peaks in the XRD *() -2()* spectra confinns that all 8 films are c-axis oriented as expected. The B2O peaks are barely visible as the B2O concentration is fairly smaU. However, the presence of the BZO has been confim1ed from lhe observation of the (200),(220), and (400) peaks at 21.339°, 30.412°, and 43.429°, respectively, in the original *lJ* -2/Jspectra for these samples [44]. The c-lat1ice constants estimated from the YBCO (001) peaks for the 2, 4, 6, and 8% SL films are I1.746 A, I1.758 A, 11.738 A, and 11.718 A. respec-tively, as shown in Table SI (Supporting Material), which are significantly larger than that of I J.67 A for undoped YBCO as expected from the tensile strained YBCO lattice due to B2O doping [26), [30), [45]. Interestingly, comparable or slightly larger c-lattice constanlS

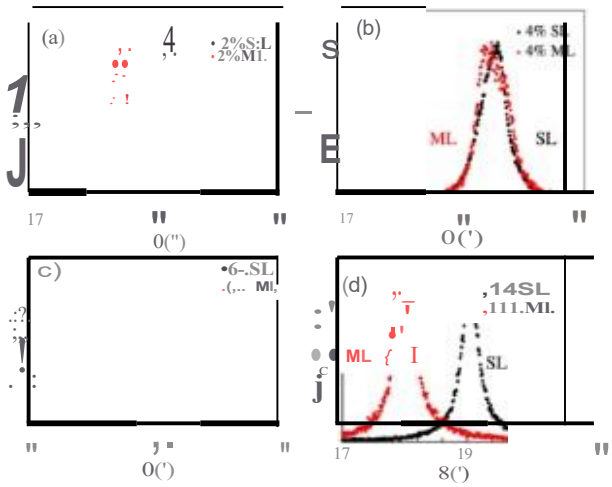


Fig. 4. XRD (005) rod:ing cums of YBCO taken on (a) 2% SL and ML (b) (a) 4% SL and ML (c) 6% SL and ML (a) 8% SL and ML BZOJYBCO **nanocomposite films.**

or 11.766 A, 11.725 A, 11.766 A, and 11.726 A were observed, respectively, on 2, 4, 6, a11d 8% ML films (see Table SJ), which is consistenl LOthe c-axis enlargemenl to up LO 1.26 nm observed in 2% ML films and is attributed to the fonnation of stacking faultson the YBCO's Cu-O planesdue to Ca/Cu substation near the BZO ID-APCIYBCO interface[32]. Fig.4{a}-(d}compares the (005) YBCO rocking curves taken on the 2--S% SL (black) and ML samples (red) BZO/YBCO nanocomposite films. The full width at half maximum (FWHM) values are 0.356', 0.533', 0.242', and 0.336' for 2, 4, 6, and 8% SL films, respectively, in TableSI (Supporting Information). ComparJble FWHM values oro.322·. 0.639°, 0.380', and0.467° can be seen for2, 4, 6, and 8% ML films, respectively. These FWHM valuesdoesnot show any trend withchanging 820 concentration for bolh SL and ML films. Jhaet al. [46] observed sirnilarFWHM values in lhe range or 0.14'-0.46' in (BSO+$Y_2$0s)IYBCO nanocomposite films with systematically increasing BSO ID-APCs concentrations. Gautam el al. [47] observed a similar trend with BHO/YBCO nanocomposite films with BHO doping concentration varied from 2% to 6%. In addition, a similar FWHM trend was also reported in (BZO + $Y_2O_3$)/YBCO nanocomposile film with a systematic variation or BZOdoping up to 6% [48]. Interestingly, the **(005)** peak location for the ML samples are either comparable on slightly smaller than that of their SL counterpart's, as shown in Fig. 4. This trend has been observed in most ML and SL sample sets and suggests the slightly larger c-axis lattice constants in ML samples possibly due to the elongation of the c-axis near the stacking faults fonned primarily near the BZO I D-APC/YBCO interface. However, the opposite trend of comparable or a slightly smaller c-axis lattice constants in ML samples as compared to their SL counterparts' has also beenobserved on some samplesets,suggesting the ca-ctiffusion induced microstn1cturemodification may **be** dictated by sample fabrication conditions, which may experience a subtle variation run to run.ln addition, lhe currenl PLOcondition wasoptimized for 6% ML samples, which means further optirni1.ationof PLD conditions may be needed for the ML films with other BZO doping levels. ll is noted that the XRD measured c-axis lattice constants are considerably smaller than that by TEM measured primarily near the BZO ID-APCIYBCO interface. We, lherefore, argue the Ca/Cu substitution on the Cu-O planes of YBCO occurs mostly near the BZO ID-APC/YBCO interface where tensile strain is the highest before the substitution.

The critical temperaLure (Tc) values were determined from the R-T curve measurement on the SL and ML rilms. The *T,* values of 89.4 K, 87.4 **K,** 86.9 **K,** and 86.5 K, respectively, were observed on the 2, 4, *6,* and 8% SL films as summarized in Table SI and plotted in Figure S2 (Supporting Material). In addition,the *Tc* valuesof87.5K,85.5K,84.0K,and85.5 K were observed, respectively, for2%, on lhe4%, 6%, and 8% ML films (seeTable SI, Supporting Material). The monoLOnic decreasing *T,* values with increasing BZO doping in the case of SL films (black) is shownin FigureS2 (Supporting Material) is consistent with the literature [24], [49], [50], [51], which is attributed to the increasing strain field overlap as the spacing between BZO 1O-APCs reduces from 20 run at 2%, to 15 nm at 4%, 12 nm at 6%, and 10 nm al 8% of BZO doping [29], [50]. Horide et al. [30] and Cantoni et al. (29] observed that the YBCO column of a thickness of 10-20 run around a BZO ID-APC is strained and oxygen deficient, resulling indegraded superconductivity in the strained YBCO and, hence, lower *T,* al higher BZO doping due to strain field overlap. Interestingly, this *T,* versus BZO doping trend is no longer the case in the 82O/YBCO ML (red} films (Figure S2, Supporting Malerial). Allhough lhe *Tc* values in the ML samples are further reduced as compared to their SL counterparts' most probably due to the ca diffusion and Ca/Y substitution in the YBCO matrix from the spacer layers. Interestingly, the *Tc*drop in 8% MLsample iscomparable to 4% ML and smaller than that in 6% ML sample. ll may be plausible to argue that the negative impact of the strain field overlapin 8% BZO/YBCO samples may be reduced by using the ML structure sinceoxygen deficiency in Lhe YBCO columns around the BZO ID-APCs would be reduced considerably when the BZO/YBCO lattice mismatch is much reduced [44].

The benefit of the improved BZO ID-APC/YBCO interface is illustrated in the enhanced pinning efficiency of the BZO 1O-APCs in the ML samples. Fig. 5(a}-(d) compares theJc(BJ curves of lhe 2--S% SL (open) and ML (solid) films al *BIie* in the field range or 0-9 T at a temperature or 65 K (black) and 77 K (red). At 65 K at which the *Tc* effect may be negligible, all ML films exhibit higher *Jc* values in the entire field range as compared lo their SL counterparts'. For example, al *65* K, a *Jc* enhancement of 1.71, 1.73, and 2.60 times is observed on the 2% ML film at 3 T, *5* T, and 9 T, respectively, over that of the 2% SL film. A similar trend can be observed on samples with higher BZO doping. The *J,* enhancement peakson the 6% ML film with 2.64, 2.91, and 4.35 times enhancement at 3 T, *5* T, and 9 T, respectively, with respect 10 lhal for the6% SL sample. At 8% ML film, enhancement of 1.71, 1.55, and I.IO times is observed. Al the higher temperatureof77 K, the *Jc*enhancement in ML films is not as significant possibly due to the *Tc* effect. Interestingly, a significanl enhancement has been observed in self-field *Jc* values at 77 K for ML films. For example, the self-field *Jc* of 1.72 MNcm$^2$ for 2% ML film is 1.86 times

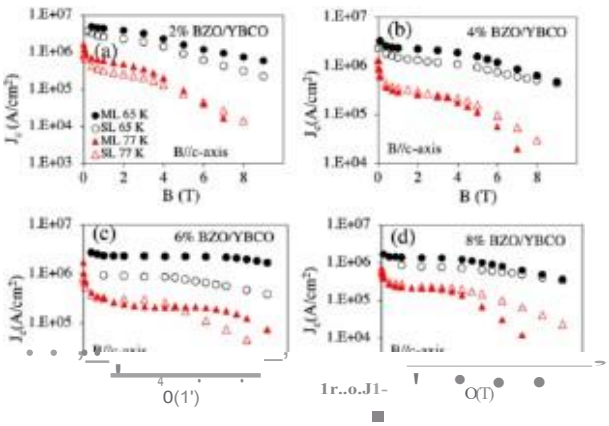


Fig. S. Comparisons of J,(B/cumsof1be(a) 2%SL(open)and ML(solid (b) 4% SL and ML (c) 6% SL and ML. and (d) 8% SL and ML BZOIYBCO **nanocomposite films. The *le* measuremen1were taken at *8//c*. The plots are denoted bycircles for6SK andtriangle.-. for*n* K *lc,{.H)* cur.-cs.**

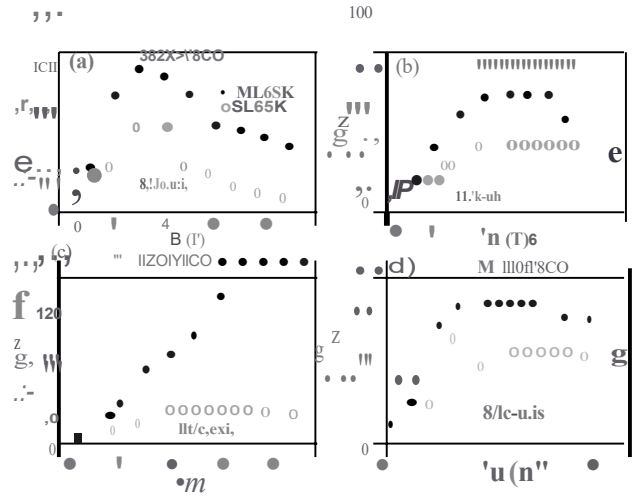


Fig. 6. *F,* versusBplolSfor(a)2% SLandML(b)4%SLandML(c) 6%SL **and ML (d) 8%SL and ML na.nocompo.site films a165 K. The solids symbols are forthe ML films andOfX'n arcforI.heSL films rc.-.pecti,•ely.**

higher than iLS SL counterparl. Similarly, an enhancement of 1.03, 2.45, and 1.25times is observed in 4% (1.44 MA/cm$^2$), 6% (2.17 MNcm$^2$), and8%(0.86 MNcm$^2$) MLfilms, respectively, over their SL counterparlS'.This enhancement, together with a reduction of *Tc* in lhe MLsamples, may beassociated to lhe hole doping (overdoping) effect of !he caon YBCO in!he ML films, especially where the strain field is not strong such that Ca/Y substitution is preferred since these two ions has almost equal radii [42], [43]. The holeoverdoing has been reported to resull in a reduction in*Tc* and an increase in *Jc* valuessignificantly in self-field or low fields. Forexrunple, Daniels et al. (42) reported 40% *I*c enhancement in 0.3 Ca doped YBCO samples (thickness ~ 228 nm, *Tc* = 78 K) at 44 K and 0-3 T magnetic field range. Since bolh moderately reduced *Tc* and increased *Jc* in self-field and low fields were observed in lhe BZO/YBCO ML samples, we hypothesize the ML samples might be moderately overdoped. Neverlheless, the enhanced pinning in higher fields to the improved pinoing efficiency of BZO ID-APCs with a coherent BZO/YBCO interface (44).

The *Fp(B)* curves for the same 2--8% concentrations of SL (open) and ML (solid) BZO/YBCO films in Fig. *5* at 65 K (with negligible *Tc* effect) are shown in Fig. 6(a)-(d). The *Fp(B)* curves have a characteristic inverted bell shape for bolh the SL and ML films and the peak of *Fp* (Fp,maxl locates at Bmax on each curve. The enhanced Jc(B) leads to an enhanced Fp(B) in the ML films at 65 K for all BZO doping of 2-8% investigated in!hisarticle.Specifically, al a temperature of 65 K, higher *Fp* values are observed on all ML films in the entire field range of 9 T. Al 2% BZO doping [see Fig. 6(a)J, lhe *F*p,max's for the ML and SL films located approximately at the srune locations of Bmax ~3.0 T despite an enhanced Fp,max value by approximately 71% from ~57.0 GN/m$^3$ for the 2% SL film 10 ~97.7 GN/m$^3$ for the 2% ML film. The above *Fp,max* value for 2% ML film is higher than the ~80 GN/m$^3$ of the 2% BHO/YBCO SL film (20) and ~ 36 GN/m$^3$ of the 2% BSO/YBCO SL film (46). It should be noted lhat the *Fp,ma.x* value for the 2% SL BZO/YBCO film is comparable 10 !hat reported in the literatures (16). Similarly, an enhanced Fp,max by approximately 67% from ~47.0GN/m$^3$ for lhe4%SL film to ~78.2 GN/m$^3$ for !he 4% ML film can be observed in Fig.6(b). Both Bmax and Fp,max are dramatically enhanced in the 6% ML film as compared lo its SL counterpart's. In fact, the enhanced *Bmax* ~8.0T in the6% ML film is 33.4% higher than thatof the 6% SL film. In addition, lhe Fp,max ~157.7 GN/m$^3$ in the 6% ML film is 296% higher than that of its SL counterpart's. The enhancement reduces at higher BZO doping. Specifically, the *FP,"""""*~50.2 GN/m$^3$ in the 8% ML film is 47.0% higher than !hat of !he 8% SL film. In contrast to the other ML films, 8% ML film has a lower Bmax value of *5* T compared to 6 T for the SL counterparts, which needs further investigations. In SL films, !he *Fp,max* value decreases monotonically from 57.0 GN/m$^3$ to 34.0GN/m$^3$ with increasing BZO concentration from2% to 8% (see Table SI, Supporting Material) (16). This is expected as strain field overlap becomes more significant in BZO/YBCO SL films wilh higher BZO concentrations (29]. In contrast, this pattern is not followed in the BZO/YBCO ML samples, which indicates thattheincreasing strain fieldoverlapwithBZO concentration is no longer !he case with the reduction of the 820 ID-APC/YBCO interface strain. This, together with the overdll enhanced *Fp,mM* values, illustrates the important effect of lhe BZO I D-APC/YBCO interface on the pinning efficiency oftheBZO ID-APCs and suggests further enhancement may be possible throughoptimization of Ca diffusion in the MLsamples al different BZO concentrations.

Fig. 7 compares the Jc(//) forthe2--8% BZO/YBCOSL(open) and ML (solid) films at magnetic fields of *5* T (black) and 9 T (red) al 65 K. *Je* enhancement can be observed in the ML samples over!heir SL counterparts' at different magnetic field orientations away from *BIie-axis*. This suggests the benefit of improving the BZO ID-APC/YBCO interface for restoralion of !he pristine pinning efficiency of the BZO ID-APCs can extend to a wide range of the B-field orientations away from *BIie-axis (0* = 0°*)*. Al *5* T, the 2-8% ML films show higher $J_{c(0)}$ in the enlire angular rnnge as compared lo their SL counterparlS over the entire angular range of 0-90°. Al 45°, !he *Jc* in the 2% ML film is 1.8 and I.7 times, respectively, of that of its SL

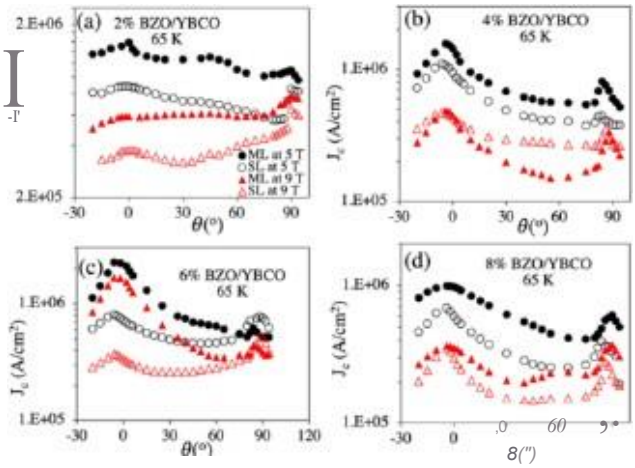


**Mg. 7. lc(8) curves messurod al 6S K, and *5* T (block) !ind 9 T (red) on** (a) 2% SL (open) and ML(solid). (b) 4% SL and ML. (c) 6% SL snd ML, and (d)8% SLand MLB20/YBCO uauocomposite 6Jms.

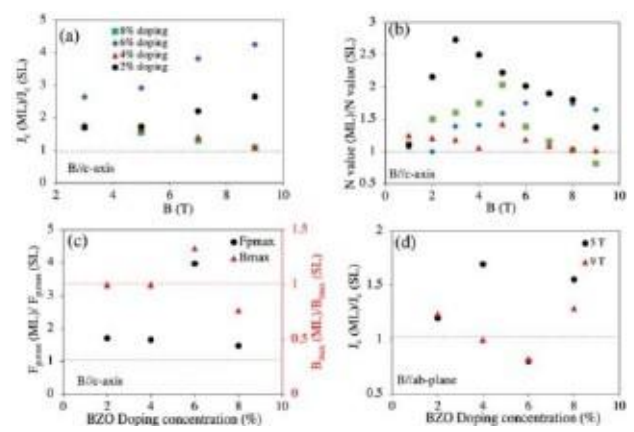


Fig. 8. {a) Plot of *J,* (ML)/J, (SL) as a function or magnooc 6eld for 2. 4. 6, and 8% 820 doping at 65 K in the B-field range of :l-9T applied along **Biledirection.(b) Norm:ili:,.ed N(ML)/N(SL) value versIL,; B-fieldcurves for2% (black),4% (red), 6% (blue), and8% (green) BZO/YBOO nanooomposite lilms.** (c) **Noonal.ized Fr,.mv. (ML)fFp.m:u:(SL)(left y-axis) at1dBm<;t.x (ML)/Bmax** (SL) (right y-axis)as function of BZOdoping, (d)Plot of*J, (ML)IJ,*(SL) asa function of the BZOdoping at 5 T(black)and 9T (red) applied a l *8/fab* plane.

counterpart's at *5* T and 9 T. Similarly, enhancement factors of 1.4 and 2.5 were observed in 4% ML sample with respect to its SL counterpart's at the samecondition. Contrary to the2% films, the 4% SL sample outperforms the 4% ML sample in lhe angular rangebetween I0-85° at9 T measurement [see Fig. 7(b)], which may be caused by some unknown effect in *J*c(fJ) measnrement of lhe 4% ML sample. On *6%* ML sample, the *Je({J)* enhances greally at both *5* T and 9 T over the entire angular range, as depicted in Fig. 7(c). The enhancement of 1.50 and 1.57 times at fields of *5* T and 9 T is observed in *Jc* value at *(J* =45°. The 8% ML film also has a *J,* enhancement over its SL counterpart's over the entire angular range at *5* T and 9 T. Al *(}* =45°, the *Jc* enhancement factors of I.9 and I.4 are observed on the ML fihn.

Fig. 8(a) depicts lhe J.(ML)/J.(SL) ratio versus B-field in the range of 3-9 T curves at *65* K for the four sets of 2, 4, 6, and 8% B2O/YBCO SL and ML samples. The values are compared at 65 Kat which *Tc* effect is the minimum. All four cnrvesare abovethe horizontal line al/ *c(ML)/J* c(SL) =I, which is expected from the enhanced pinning in lhe ML samples. However, the *J*,(ML)/J ,(SL) for the 2% and *6%* films follow an opposite trend to that for the4% and8% films. In the Fonner, the *J*c(ML)IJ c(SL) increaseswith increasing B-field wbilein the latter it decreases wilh lhe B-field. Due lo lhe opposite trends, the highest Jc(ML)/Jc(SL) of2.65 and 4.25 are obtained at 9 T for the2% and 6% films. In contrast, the 4% and 8% ML films showthemaximum$J_0$(ML)/$J_0$(SL)of 1.70and 1.71althelowesl field of3 T. IIshould be noted that the opposite trends in the four setsof theSL and ML samples of clitferent B2O concentrations are not expecled. which means fnrther investigation is needed to confinn the ML samples of different BZO concentrations are made in optimal conditions.

The enhanced pinning in the ML samples can be further confirmed in lhe higher N values observed in lhe ML samples as compared to theirSL counterparts'.To quantify this comparison, the normalized N(ML)/N(SL) is shown as function of the 8-field for lhe 2% (black), 4% (red) *6%* (blue), and 8% (green) films al 65 Kand B//c [see Fig. 8(b)]. Almost all N(ML)/N(SL) values are above the horizontal line at N(ML)/N(SL) = I as expected. ll should be noted lhal lhe N value is proportional to lhe pinning potentials of Lhe BZO I D-APCs in SL and ML films. All four curves show a peaJc near their Bmax values, similar to the *F*p vs *B* plots shown in Fig. 6. Forexample, the peak of the normalized N for the 2% samples is around ~2.5 at ~3 T. For the 4%, 6%, and 8% films, the peak N(ML)/N(SL) values are around~ 1.43 al *5* T, ~ 1.9 at 7.0 T, and ~2 al *5* T, respectively. Considering the pinning potential is proportional to the radial derivative of the pinning energy at lhe B2O/YBCO interface, Blatter el al. [52] enhanced pinning potential in the ML samples may be attributed to the much less degradedsuperconductivityin YBCO around the B2O ID-APCs through the coherent BZO/YBCO interface.

Fig. 8(c) compares Lhe *Fp,max* (ML)/Fp,max (SL) (black, to left Y-axis) and Bmax (ML)/Bmax (SL) (red, to right Y-axis) values at different B2O doping of 2-8% at*65* K. The enhanced pinning in the ML samples as compared to their SL counterparts' is illustrated in the normalized *Fp,ma:x* values exceeding I (black dashed line) for all B2O doping in lhe rnnge of2-8%. Interestingly, the highest enhaneement occurs Lo the 6% ML samples with the Fp,ma:x(ML)/Fp,max (SL)~ 3.96. The *Bmax* (ML)/Bma:x(SL) plot follows the same trend of the normalized *Fp,m-.u* wilh lhe peak enhancement of ~1.33 on lhe *6%* ML sample. While understanding the trend requires further investigation, especially by optimizing the sample growth at each differenl B2O doping, the effecl of the strain-field overlap al variable BZO doping should also be considered due to their influenceon Ca diffusion and substitmion. Fig.8(d) exhibits the $J_0$ (ML)/Jc (SL)at5 T (black) and 9 T (red) *(Bl/ab*plane) for the four sets of BZO/YBCO nanocomposile films of BZO doping of 2-8%. Interestingly, the two curves show an opposite trend lo that in Fig. 8(c) with 6% ML sample having the lowest *Jc (ML)IJ*$_0$(SL)~ 0.8 al both fields. Since higher *Jc* at *Bl/ab* plane reflects the integrity of the *ab* planes in the nanocomposite films assuming the inserted APCs may dismpt the flatness of the *ab*

plane, controlling the strain field is important 10 the ultimate design of high-performance nanocomposite films.

h should be mentioned l.hal the Fpma.x and Jc enhancement dependence on BZO doping shown in Fig. 8(c) and (d) appear somehow stochastic. Although multiple samples at difl'erent BZO doping levels were studied, in this article, and all ML samples exhibited enhanced pinning, the same PLO fabrication condition optimized for 6% ML samples may need to be modified to achieve optimal Ca-diffusion for ML saniples with other BZO doping. This suggests it is importanl to understand !he microscopy mechanism or Ca-diffusion in the ML samples in order to achieve an optimal control of the Ca-diffusion at differeol BZO doping levels.

Through !his comparative study of the ML and SL BZO/YBCO nanocomposile films with BZO doping varied in !he samerangeof 2-8 vol.%, we haveobserved variations in the microstrucLures of the samples. One variation is the fonnation of stacking faults in the ML samples, which has been confirmed to associate to the Ca/Cu substation on the Cu-0 planes of the YBCO unit cell [44). h should be noted thal stacking faults have been reported previously 10 enhanec the pinning properties (53), [54), (55), [56). However, !he stacking faults due to the Ca/Cu substitution in ML samples differ from Lhose reported previously since noenhanced pinning at *Bl/ab* planes was observed in the ML samples. This may be explained by !he observation of !he short segments of Ca/Cu stacking faults primarily near the BZO lD-APC/YBCO int,:rface instead of through the entire film. Since !he appearance of the stacking faults leads 10 elongated c-axis lattice constant of YBCO up 10 1.26 run, !he lattice mismatch, and hence !he induced elastic strain, al the BZO I0-APC/YBCO interface is reduced from ~7.7% 10 ~l.4%. Theresults in a much less defective interface and more straightened BZO lD-APCs in the ML samples as compared to I.heir SL counterparts', both are favorable to the pinning enhancement [521.

ll should be noted that the strain field distribution in the ML samples may differ considerably from !hat in !heir SL counterparts. With the c-axis elongation due to the formation of the Ca/Cu stacking faults near lhe BZO I D-APC/YBCO interface, !he reduced BZO/YBCO lattice mismatch to ~1.4% in ML samples may lead to a minor inlerfacial strain. Away from the BZO I D-APC/YBCO interface, a reduced numberof the Ca/Cu stacking faults is expected due to a reduced Ca/Cu substation driven by I.he original interface tensile strain. This means the increasing strain field overlap with increasing BZOdoping in SL BZO/YBCO nanocomposite films may beconsiderably reduced.

## IV. CONO.USION

Using a newly developed ML approach by inserting two CaY-123 spacer layers of 10 om in thickness into 2-8 vol.% BZO/YBCO nanoeomposite films consisting of three 50 nm thick BZO/YBCO layers, considerably enhanced pinning efficiency of the BZO 10-APCs and, hence, $J_0$ have been observed in this article. At 65 K, the enhanced *FP,'''''* values al BIJ'c-axis are approximately7 I%, 67%, 296%, and47% forthe2,4, 6,and 8% ML films, respectively, higher than their SL counterparts'. The pinning enhancement in the BZO/YBCO ML films is also illustrated in their higher *Bm.,,* values by up to 33.4% than the SL counterparts'. Furthermore, the enhanced pinning efficiency of the BZO I0-APCs extends lo a broad angular range of B-field orientations away from 8//c-axis, as shown in the J,(0) plots. This article also sheds light on !he mechanism of the enhanced pinning efficiency of BZO ID-APCs in BZO/YBCO ML samples. With increased BZO doping, the increasing strain field overlap may facilitate ca ion diffusion along !he tensile strained BZO/YBCOinterface, leading to Ca/Cu substinuion on the YBCO's Cu-0 planes and the fonnalion of stacking faults. IIshould be noted thatCa/Cu substitution is energetically favorable on strongly tensile strained YBCO lattice sineCa ion is ~ 30% larger than Ca ions.The consequent c-axis enlargemenl of YBCO lattice can reduce the BZO/YBCO lattice mismatch and prevent the fonnation of defects at!he BZO/YBCO interface and therefore enhance the pinning efficiency of the BZO lD-APCs. On the hand. Ca ion diffusion into BZO/YBCO layers may also occur in places not near the BZO/YBCO interface with either reduced or no tensile strain. This means Ca/Y substitution may becomesubstantial considering Y ion hascompar•blesizetoCa ion. In this case,*Tc* reduction will bea consequence and hasbeen observed in all BZO/YBCO ML samples. This result illustrates the ML method may provide a unique tool to engineer the microstructure, especially the BZO I0-APC/YBCO interface, for the optimal pinning efficiency of BZO ID-APCs.

## REFERENCES


[ 11 G. Alecu, ·-crystal .structures ofsomebigh-te.mpernluresupe.rconductoni:,'' *Ronuinian Rtp. Phys..* vol. *S6*.no. 3, pp. 404-412. 2004.

(2) A. Mourac-hkine. *Room-Ttmperature Supen oJJducrMty.* Cambridge. U.K.: Cambridge International Science Publishing, 2004.

[31 X. Obmdors and T. Puig, "'Cooled conductors for P'J''''C.r applic:itions: M:iterial.s challenges,'' *Supercond.. Sci. Tt!t:luwl.,* \-OI. 27, no. 4, 2014, Art. no. 044003.

(4) S.S. *Kalsi,Applicotio,u of HighTemperature Superco,ufuc.rorsto Electric Power EquifJIMnt,* Hoboken, NJ, USA: Wiley, 2011.

(51 0. L.arbalestier ct al., •·High•Tc supercooducting m:1tcrial.s for electric powerapplkalions." in *Materials for Si,stainabfe £,tugy: A Collulion of Peer-Rei,·iewtd RtYtartlt and Rt1'it'k' Artitlts from Nature Publishing Group.* Berlin. Germany: Springer, 2011. pp,311-320.

(61 K. M:ilsumoto cl al.,-Enhancement of critical current density of YBCO films by introduction of artificial pinning cenlc. doo to the distributed nano-scaled Y203 islandsons.ubstrates:·*PhyrlcaC.Supen·o-mJ..* vol.412. pp. 1267-1271, 2004.

(7) K. Matsumoto and P. Mele, ..An.ificial pinning oenter technology co enhanoo vortex. pinning in YBCO coated conductors,'' *Supur:011d. Sci. Ttdmol..* vol.23. no. I. 2009. Art. t\0.014001.

[81 P. Mele et al.. "UIU.-high flux pinning P'''I'''rlies of BaMO3-<lopcd Y8a2Cu301-xthin films(M= Zs,Sn),"*Su rco,td.Sci.Ttchnol.*•vol.21. no. 3, 2008, Art. no. 032002.

(91 T. Hauganet al., ..Additionof n!lnoparticledi..o;persioo.,;toenhanooflu.x. pinning of the YBil'2CuaO1-x superconductor:· *Nature.* \'0I.430. no. 7002. 2004,Art. no.867-870.

[JO) J, MacManus.-Oriscoll et al.. "'Strongly enhanced current densities in superconducting oootcdoonducLorsof YBa2Cu3O7-x+BaZr03;·*Nalurtt Mattr..* ,·ol.3, no. 7. 2004. Art. no. 439-443.

(JI) T. Horide ecal.."'Matching fieldeffeccof the \'OtticesinGdBa2Cu,01-6 thin film with gold nanorods." *Supercond. Sci. Ttcluwl.,* vol. 20, no. 4. pp. 303-306.

1121 A. Goyal ct al., •·J1Tadiation-froo, columnar defects comprised of self-assembled nanodots and naoorods resulting in strongly enhanced flux-pinninginY8a2CU3O1-6films."*Supercond. Sc.l.Ttchnol.,* vol. 18, no. 11. 2005, An. no. 1533.

I 131 J. Wu, 8.Gu.utam.and V.Ogunjimi,··Pinning efficiency ofartifici:.J pinning centers in superoooductOI" nanocon1.p0Site films." in *Supen·o-tldutt Mry.* Berlin. Gennany: Springer. 2020. pp.*29-52.*

[141 J. Wu and J. Shi, ··1nter.ictivc mode.ling•synthesi.,;-charac:le:ri7.Mion approach toward.,; controllublc in silu sclf-:isscmbl)' of artificial pinning centers in RE-123 films... *Superr:ond. &i.Ttt.hnol..* vol. 30. oo. JO.2017. Art. no. I0JOOZ.

[ISi J. Z. Wud :ii.,·11,e effect of fotticc strain on the diameter of BaZr03 nanorods in epitaxial YBa2Cu301-.s film$,"' *Superr:muJ. Sci. Tech110l.,* rol.27. no. 4. 2014.Art. no. 044010.

(16) S. H. Wee et al., "Engineering nanocolumnar defect configurations for optimized vortex pinning inhigh temperature superconducting nanocomposite wire. ·•*Sci.Ht!p.,* ,-ol. 3, 2013, Art. no.23IO.

(17) S. Miura el al. "'Strongly enhaoced irreversibility field aod flux pinning force density in SmBa2CU30 y-coated conductors with \IX'll-aligned BaHfO3 nanorods," *Appl. Phys. Exp.,* \'0l. 10, no. 10, 2017, Art. no. 103101.

[181 S. O,en ct :ii.,··Generating mixed motphology Ba2J03 artificial pinning centers for strong and isotropic pinning in 8a2t03- Y203 double-doped YBCO thin films," *Superco,rd. Sci. Technol.,* vol. 30, no. 12. 2017, Art. no. 125011.

[191 B.G-.autam8l al..'", 'lr.insfonnatimal dynamics of BZO!ind BHO naoorods imposed by Y20.1 naooparticles for itnproved i$'0lropic pill1ling in Y8a2Cu301-6 thin films.'" *AIPAdv,.·.*oL7. oo.7. 2017. *Att.* oo.07S3-08.

(20) 8. Ga.ut m et at, ..Probing me effect of interface on vortex pinning efficiency of one-dimensional B:i.Zr03 and BaHfOs artificial pinning centers in YB:12Cu30'7-,x thin films," *Appl. Phys. Utt,.,•*ol. 113, no. 21, 201&, *Atl.* IIC>. 212602.

(21] S. Chen et al., ,.Enhancement of isotropic pinning force in YBCO films with BaZt03 nanorods and Y:l03 nanopa.nicles," *IEEE Tra,u.. AppL Supur:o,id.,* \OL27, no. 4, Jun. 2017, Art.. no. 8000205.

[22) E. Galstyan. R. Pnltap. M. Paidpilli. G. Majkic. and V. Selvamanickant -'Pinning characlerislics of Zr and Hf-added REBCO coated cooductC>tS made by ad\'anced MOCVO in IOON-to-high magnetic fields," *IEEETrm,s. Appl. Supercond.,* vol. 31, no. *5,* Aug. 2021, Art. oo. 8000405.

[23] M. A. P. Sebastian ct al., ··s1udy of the Aux pinning land.-.cape of YBCO thin films with single and mixed phase additions BaM03+ 2: M =Hf. Sn, *Z,* and Z =Y2O3, Y21l." *IEEE. Tra,,s. Appl. Sup,rcond..* vol. 27, no.4,Jun.2017,An.no. 7500805.

[241 S. H. Weeet al., ..Self-assembly of nanostructured, complex, muhic!llion films \'isspontaooou.., phu.<ie separat.ion and stmin-dri\-en ordering," *Adv. Funcl. Maler:.* \'OL 23, no. 15, pp. 1912-1918, 2013.

[2S) T.Horideet at. "Influenceof matching field oncriticalcurrent deosityand irreversibility tempernture in Y8a2Cu30r films with BaM03 (M = Zr, Sn,Hf) nanorods," *Appl. Phys.t..,n.,* \'0l.103, no.8, 2016, Art. no.082601.

[261 T. Hocide et al., "Elastic strain evolution in nanocomposite structure of YBa2Cu30'7+ 8a2!03 supereoodueting films:·*Japa,,e:.·e J. Appl.Ph)•s.•* rol.53. no. 8. 2014. Art. 110. 083101.

(27) A. XuetaJ., ..Strong1yenhanced vonex pinning from4 to77 Kin magnetic fields upto31Tin I5 mol.% ZMtdded (Gd, Y)-Ba-Cu-0 superconducting tapes," *AP/..Mat r..* vol.2, no. 4, 2014, Art. no. 046111.

[28] M. Peutla el aJ••'"Effectsof nanoc:rys1aJJine targel aod columnardefoctsoo flux pinning in pore and 8aZr03-doped YBa:zCu306+ x films in fields up to 30T;• *Phys. Rev. 8,* rol.75, oo. 18,2007, Art. no. 184524.

[291 C. Cmtoni et al..,-st.min-driven ox.ygcn deficiency in self--,asscmblcd, nWlOSlructured. composite oxide films." *ACS NanQ.* ,·oL *S.* no. 6, pp. 478 789. 201I.

(30) T. Horide et al., "'Strocroral e\'olution induced by interfacial Janice mismaLch in self-organi1.ed Y8a'20l301-&nanocomposite film," *ACS Nano,* vol.11,oo.2,pp.1180-1788,2017.

[31) P. Mele el aJ•• *Supertonduc-ti▶ ·ity: Fl'(Jm !tftuerials Scie11c-e to Prac-tic'lJI Applicasions.* Berlin. Germany: Springer,'2019.

[321 V. Ogunjimi ct al., •'Enh!!ncing Magnett<: pinning by BaZI03nanorods fonning coherenl interface by strain irocted Ct-Doping YBlt1Cu307-x nWlooomposite films." *Supen ond. Sci. Ttclttol..* ,·ot 34. no. JO. 2021. *Atl.* IIO. 104002.

(33) R. Kiteet al., "'Enhanced cu1Tent transpo11 atgrain boundaries in high-Tc superconductors," *Nalu",* vol.435, no. 7041, pp.475-47&, *2005.*

[34] T.He>rideet al.. "Hybrid artificial pinning centers or elongated-naoorods andsegi:nented-nanorods ill YBa2Cu307 films:·*Supertond. Sci.Ttc-fmQf.•* ,ol.*29,*2016, Art. oo. 105010.

(351 M.Malmi\•irlaelal.,··EnhancedOux pinning YBOO muhifoyer films wilh BCO nanodoL'i segmenled BZO nanorods," *Sci. Rep.,* \'Ol. 7, no. I, 2017, *Att.*no. 14682.

(36) M.A. P.Sebastian et al., "Study flux pinning landscape YBCO thin films with sing'8 mixed phase additions BaM03+ Z: M= Hf.Sn, Zr and Z= Y203, Y21l," *IEEE Trans. Appl. Superco11d,* \'Ol. 27, no. 4, Jun. 2017, Art. no. **7500805.**

(37) X. Wang e1 al., "F.Jiminating thick.ness dependence of critical current density in Y8a2Cu30$_7$_x 61ms with aligned BaZrO3 nanorods,"*J. AppL Phy:r.,* vol.108, no. 11, 2010, Art. no. I13911.

[38] F. J. Baca etal.. "'Interactive growth effectsor rare arth naooparticles on nanorod fon:nation in Y8a2CU30x thinfilms." *A<.hi F11,1C't.Matt-r:.*vol.23. no. 38, pp. 4826-4831, 2013.

(391 D.R. Askcland cl al., *Tht! Scienu a11d F.t1gi.,1eering,,f Male.rials.* Berlin, Germany: Springer. 2003.

[40] D. W. ruchersoo and W. *£.Lee.ModemCe,a,nj(:Ertgh1.uring: Properlit"S. Processi,1g, mulUse in Design.* Boca Raton, FL,USA: CRC Press, 2018.

(41J V. Sharma et at, "Machine learning substitutionaJ defec1 formation ene,g.les in AB03 penwstitcs." *J. Appl. Phys.,* vol. 128, no. 3, 2020, Art. no. 034902.

[42) G. A. Daniels. A. Gurevich.. and D. C. Latbalestier. "'Improved strong magnetic field performance of low angle grain boundaries of calcium !ind oxygen overdoped YBazCu3C>,c," *Appl. Phys.. I.ell.,* vol. 77, no. 20, pp.3251-3253, **2000.**

[43) A. Schtnehl el al.•"Doping-induced enhancement of the critical cutrent.s of grainboundaries in Y8a2Cu,3Cn-a," *£PL(Europlryslcs lea.J.* \'OI.47, no. l, 1999,Art. oo. 110.

(441 J. Z. Wu et al., ··Enabling coherent BaZro.3 nanocod-.!YBazCu301-x interface through dynamic lattice enlarge.me11t ill vettical epilAx.y of 8aZr03N8a20l307_x nanooomposites:· *Superrond. St'i. Ttt·hn(Jf..* vol. 35,*202Z.*An. no. 034001.

(451 R. Ca\'a et al., ··structural anomalies, oxygen ordering supcrcondut..1.ivily oxygendeficient 8 Y0.30x," *Pltysica C, S11permnd.,* \UI. 165, no. *516,* pp.419-433, 1990.

(46) A. K. Jha. et al.. "Th.iJoring vortex pinning strength YBCO chin films by systematicincorporation hybrid artificial pinningcenters," *Supercond. Sci. T«h110I.,* vol.2&,oo. 11, 2015, Art. no. I14004.

(471 B. Gautam ct al., -Microscopic ad:aptation of BaHf03 and Y203 artificial pinning centers foe strong Md isotropic pinning landsc!!pe in YBa2Cu$_3$01-x thin films.··*Superr:ond. Sci.Ttc-fmQf.•* \'OL 31.no. 2. 2018. Art.no. 025008.

(48) M.Sebas1ian et at, "Comparison study of the flux pinning enhancement of YBCO superconductor wilh 820 and BZD+ Y203 mi.xed phase additions." ill *Proc. /OPConf Ser:,Mattr. Sci. Eng.•* 2017.

[49) P. Mele et al., "Systematic study Ba.Sn03insertion effect prope.rt.ies YB32CU301-x films prepared by poised laser ablation," *Supercond. Sci. T«hnol.,* vol.21, oo. 12, 2008, Art. no. 125017.

(501 M. Peoria cl al-.,op1.imi:r.ation BaZrC>J concentration YBCO films prepared bypulsed Jase,deposition:·*Su n.·ond.Sci. Technol..* vol. 19.no.8. An.. no. 767.

(51J A. Ichinoseet at, ..MtCrostructurescritical current densities YBCO films containing stcucluro-controlled BaZr0:3 nnnomd..,," *Supermnd. Sci.Technol..* \'OL 20.oo. 12. 2007. Art. no.1144.

[S2] G. Blatter et al.. "CVooices in high-te,:nperature superconduclors:· *Rev. Mod,mPl1ys..* rol.66, no.4, pp. 1125-1388, 1994.

(531 J. Gutierrezct al., "'7heroleof stacking foulL., inthe criticalcurren.tdcnsily of MOD films lhrough a thtCkooss dependence study," *Su rr:mul. Sci. Tec-111101..* rol.*22.*no. I. 2008.Art.no. 015022.

(54) T. Horide et at, ••Nonlocal se1f--0rganiza.tionof k>ng stacking faults from highlyst.mined n!lnocomposite filmof complexoxide." *Phys. Rev.Matl'.r.,* vol.3, no. I, 2019, Art. no. 013403.

[SS] T. Horideet al•. -'Combined effecl naoorod staddng fault for improving nanorod interfuce YBa2Cli,3°'7-a nanooomposite films.'" *S rrond. Sci. r,chrllJI.,*rol. 33, oo. 11, Z020, Art. no. 115001.

(561 A. Llocdes el al., ..Nan05Calestrain-induced pairsuppress:ion as a vortex.-pio.ning mec.banism in high-(emperature superoe>nductors:·*Natun Mater:.* vol. 11.no. 4. pp. 329-336. 2012.